Headloss in two phase flow of water and steam in geothermal gathering pipe systems

Ingi Heimisson

Faculty of Industrial Engineering, Mechanical Engineering and Computer Science
University of Iceland
2014

HEADLOSS IN TWO PHASE FLOW OF WATER AND STEAM IN GEOTHERMAL GATHERING PIPE SYSTEMS

Ingi Heimisson

60 ECTS thesis submitted in partial fulfillment of a
Magister Scientiarum degree in Mechanical Engineering

Advisor
Halldór Pálsson
Guðrún Sævarsdóttir

Faculty of Industrial Engineering, Mechanical Engineering and Computer Science
School of Engineering and Natural Sciences
University of Iceland
Reykjavik, June 2014

Headloss in two phase flow of water and steam in geothermal gathering pipe systems
Headloss in two phase flow of water and steam in geothermal gathering pipe systems
60 ECTS thesis submitted in partial fulfillment of a M.Sc. degree in Mechanical Engineering

Faculty of Industrial Engineering, Mechanical Engineering and Computer Science
School of Engineering and Natural Sciences
University of Iceland
VRII, Hjarðarhaga 2-6
107, Reykjavík, Reykjavik
Iceland(Þorbjörn Karlsson, 1979)

Telephone: 525 4000

Printing: Háskólaprent, Fálkagata 2, 107 Reykjavík
Reykjavik, Iceland, June 2014

Abstract

The goal of this project is to measure pressure drop in gathering pipelines in a geothermal power plant and compare the measurements to predicted pressure drop according to known pressure drop models. The best suited model is found for the measurements. The effect of changing steam quality and roughness on the models is discussed. Most of the known models are emperical and only valid for the range they were made for. Orkuveita Reykjavíkur provided the physical data for the gathering pipes and Mannvit h.f. provided layout data. 6 gathering pipelines were measured at the upper region of Hellisheiði Power plant. Not all measurements nor the provided data were made at the same time which might not give the most accurate comparison of models with the measured data.
The model with lowest combined average error and spread was Beattie model. Three others models predicted a lower average error but these models gave higher combined average error and spread. Since the known models were made in pipes that have much smaller diameter and less roughness a new model with diameter and roughness closer to the geothermal gathering pipes is preferred to be able to calculate the pressure drop accurately.

Útdráttur

Markmið þessa verkefnis er að mæla þrýstifall í safnæðum jarðvarmavirkjunar og bera saman við þekkt þrýstifalls líkön. Það líkan sem passar best við mæld gildi er fundið. Áhrif af breytilegu massahlutfalli og hrýfi á líkön eru skoðuð. Flest líkön eru emperísk og virka best fyrir afmarkað svið sem þau voru hönnuð fyrir. Orkuveita Reykjavíkur útvegaði flæðisgögn safnæðana og Mannvit h.f. útvegaði landfræðilega legu safnæðana. Mælingar voru gerðar á 6 safnæðum á efra svæði Hellisheiðarvirkjunar. Hvorki mælingar né gögn frá Orkuveitunni voru gerðar á sama tíma sem gæti gefið ónákvæman samanburð við líkön.
Það líkan sem var með lægsta meðaltal skekkju og dreifni var Beattie líkan. 3 önnur líkön gáfu lægri skekkju en dreifnin var meiri sem gaf hærri samanlagða skekkju og dreifni. Þar sem þekktu líkönin voru sett fram með pípum með töluvert lægra þvermál og hrýfi þá er ráðlagt að gera nýtt líkan, sem styður stærra þvermál og meira hrýfi, til að geta reiknað þrýstifall með meiri nákvæmni.

Contents

List of Figures

List of Tables

Nomenclature

A	Area inside a pipe, m^2
A_g	Area of pipe where only gas exists, m^2
A_f	Area of pipe where only fluid exists, m^2
D	Inner diameter of pipe, m
f	Friction factor
g	Acceleration due to gravity, m/s^2
h	Enthalpy, J/kg
h_g	Enthalpy of gas phase in mixture, J/kg
h_f	Enthalpy of fluid phase in mixture, J/kg
$\dot{Q}$	Total mass flow, kg/s
$\dot{m}_g$	Mass flow of steam, kg/s
$\dot{m}_f$	Mass flow of fluid, kg/s
p	Pressure, Pa
S	Slip ratio
u	Velocity, m/s

u_g	Average velocity of gas phase, m/s
u_f	Average velocity of fluid phase, m/s
u_m	Average velocity of mixture, m/s
Re	Reynolds number
Re_g	Reynolds number for gas phase
Re_f	Reynolds number for fluid phase
T	Temperature
x	Steam quality
z	Height difference between high and lowpoint of pipe route
α	Void fraction
μ_g	Dynamic viscosity of gas phase, Pa.s
μ_f	Dynamic viscosity of fluid phase, Pa.s
Φ	Friction correction factor
ρ	Density, Kg/m^3
ρ_g	Density of gas phase, Kg/m^3
ρ_f	Density of fluid phase, Kg/m^3
ρ_m	Density of mixture, Kg/m^3
L	Length of pipe, m
ϵ	Roughness of pipe, mm

Fr	Froude number
We	Weber number
σ	Surface tension, N/m
X	Lockhart-Martinell parameter
B	Barozcy correction factor
Γ	Chisholm physical property coefficient
G	Mass flux, Kg/m^2s

1 Introduction

Geothermal energy is frequently used directly or for production of electricity. Direct use is used to heat up buildings, swimming pools, fish farms and other industries where heat is needed. Electricity is produced by a generator, which is powered by a steam turbine. The steam to the turbine is separated from a high temperature geothermal fluid. That kind of power plant is called a flash steam power plant.

Dry steam power plants and binary cycle power plants are also used. Dry steam power plants are the simplest design. Then no separation is performed on the geothermal fluid before the turbine. Binary cycle power plants are the most recent technology. A warm geothermal fluid, is used to heat up a secondary fluid with a much lower boiling point than water. That causes the secondary fluid to flash into steam which turns the turbine.

Flash steam power plants are most common in Iceland. In 2013 installed geothermal electric capacity in Iceland was 664 MW which is 30% of Iceland's total electricity production. The transport pipelines, from the borehole to separation stations, consists of two phases, water and steam. This makes it hard to simulate since there are many parameters and conditions that intertwine, for example turbulence efficiency, flow regimes, pipe roughness, mass flow of water and steam and therefore the velocity of the two phases. The steam pressure and the mass flow to the turbine control the power outlet so it is important to minimize the pressure drop in the transport pipelines from the boreholes to the power house.

The aim of this project is to measure pressure drop in transport pipelines in the upper region of Hellisheiði power plant and compare measurements with known pressure drop models and choose a model which suits measured data.

2 Geothermal Energy

2.1 Geothermal Power Plants

Geothermal power plants can be both heat and power plants. The geothermal fluid is then used for both electricity generation and heat purpose. Geothermal fluids flows from reservoir to the well. There it boils on its way up the well cause of pressure drop in the well. The fluid runs in gathering pipelines, gathered from several wells, into a steam separator. There the steam and fluid separates before the final separation in the mist separator, which takes the last droplets in the steam before going into the turbine. A generator is connected to the outlet of the turbine which generate electricity for the consumer. Then the steam goes into a condenser where it cools down and is condensed. The condensed steam is used to heat up cold water for district use.

2.2 Hellisheiði power plant

There are 7 geothermal power plants in Iceland. Cycle types vary from single flash, double flash and Kalina. Geothermal heating meets the heating and hot water requirements of approximately 87 percent of all buildings in Iceland.

The data and measurements in this project were made at Hellisheiði Power plant. The plant is in ownership of Orkuveita Reykjavíkur. It is stationed at Hengill, southwest of Iceland. The plant has installed capacity of $303MWe$ with $133MWt$. It has $6 \times 45MW$ high pressure turbines and $1 \times 33MW$ low pressure turbine in operation.

3 Theory

In this chapter single and two phase flow governing equations will be discussed. A comparison of different void fraction, friction factor, friction correction factor for straight pipes and for bends will also be discussed.

3.1 Flow modeling

Flow modeling of two phase flow can be divided into two categories, homogenous and separate flow models. The homogenous flow model assumes that the two phases, water and steam, flow at the same velocity. Separate flow models assume that the two phases travel at a different velocity. Since separate flow models are most empirical and done with small diameter pipes, scaling these models may not give accurate results in large diameter pipes. (Pálsson, 2012)

There are three model types used to analyze two phase flow. Empirical models, semi-analytical models and numerical models. Since there is limited knowledge of two phase flow, most models consist at some extend empirical correlation. These models are

1. Empirical models are mostly based on series of experiments. Since two phase flow is very sensitive to properties changes these models are mostly usable for the conditions they were correlated on.

2. Semi-analytical methods, also called mechanistic method, uses physical phenomenon and takes most important effects into calculations but neglecting other less important.

3. Numerical modeling is the most complex method to solve multi dimensional equations for multiphase flow. Numerical method is time consuming and complex and will not be examined in this project.

3.2 Single Phase flow

Single phase flow is where only one phase is present in the pipe. This phase can be liquid or steam. The primary variables in single phase flow simulations are, velocity, pressure, enthalpy and density.

Continuity equation

The continuity equation derives from the conservation of mass.

$$\frac{d}{dz}(\dot{m}) = 0 \tag{3.1}$$

The diameter stays constant so equation 3.1 can be written in terms of density.

$$\frac{d}{dz}(\rho u) = 0 \tag{3.2}$$

Momentum equation

The momentum equation can be divided into 4 parts.

1. Inertia change
2. Pressure change
3. Hydrostatic pressure
4. Head loss

$$\rho u \frac{du}{dz} + \frac{dp}{dz} + \rho g + \frac{\rho f}{2d}|u|u = 0 \tag{3.3}$$

Energy equation

The energy equation is derived from the first law of thermodynamics and can be divided into 4 parts.

1. Kinetic part
2. Enthalpy part
3. Potential energy
4. Heat loss

$$\dot{m}u\frac{du}{dz} + \dot{m}\frac{dh}{dz} + \dot{m}g + \dot{Q} = 0 \tag{3.4}$$

Matrix form of the equations

The continuity, energy and momentum equations can be gathered into a single system. $$\begin{bmatrix} \rho & u\frac{\partial \rho}{\partial p} & u\frac{\partial \rho}{\partial h} \\ \dot{m}u & 0 & \dot{m} \\ \rho u & 1 & 0 \end{bmatrix} \frac{d}{dz} \begin{bmatrix} u \\ p \\ h \end{bmatrix} + \begin{bmatrix} 0 \\ \dot{m}g + \dot{Q} \\ \rho g + \frac{\rho f}{2d}|u|u \end{bmatrix} = \begin{bmatrix} 0 \\ 0 \\ 0 \end{bmatrix} \quad (3.5)$$

3.3 Two Phase flow

Two phase flow is where two or more phases are present in the pipe. The primary variables in two phase flow are the same as in single phase flow with addition to void and mass fraction.

$$\dot{m}_g = \frac{h - h_f}{h_{fg}} Q_t \qquad \text{and } \dot{m}_f = Q_t - \dot{m}_g \quad (3.6)$$

$$v_g = \frac{\dot{m}_g}{\rho_g A} = \frac{x\dot{m}}{\alpha \rho_g A} \qquad \text{and } v_f = \frac{\dot{m}_f}{\rho_f A} = \frac{(1-x)\dot{m}}{(1-\alpha)\rho_f A} \quad (3.7)$$

Steam quality, x, is defined as the ratio of the mass flow of steam to the total mass flow through a given cross section at a given time:

$$x = \frac{\dot{m}_g}{\dot{m}_g + \dot{m}_f} \quad (3.8)$$

Also the steam quality can be calculated from enthalpy:

$$x_h = \frac{h - h_f}{h_g - h_f} \quad (3.9)$$

Momentum equation

The momentum equations are more complicated for two phase flow than in single phase flow, since there are two different phase velocities for inertial term. The density in the gravity part has to be averaged with respect to the void fraction, $\rho_\alpha = (1-\alpha)\rho_f + \alpha\rho_g$

$$\frac{d}{dz}(\dot{m}_f u_f + \dot{m}_g u_g) + A\frac{dp}{dz} + ((1-\alpha)\rho_f + \alpha\rho_g)gA + \Phi^2 \frac{\rho_f f A}{2d} u^2 = 0 \quad (3.10)$$

Where ϕ^2 is frictional pressure correction factor and f is friction factor, described respectably in chapters 3.6 and 3.5. To simplify the momentum equations parameter η is introduced.

$$\eta = \frac{(1-x)^2}{(1-\alpha)} + \frac{\rho_f}{\rho_g}\frac{x^2}{\alpha} \tag{3.11}$$

Then the momentum equation can be written as

$$\eta\rho_f u\frac{du}{dz} + \left(1 + \rho_f u^2\frac{\partial\eta}{\partial p} + \eta u^2\frac{\partial\rho_f}{\partial p}\right)\frac{dp}{dz} + \rho_f u^2\frac{\partial\eta}{\partial h}\frac{dh}{dz} + ((1-\alpha)\rho_f + \alpha\rho_g)g + \frac{\Phi^2\rho_f f}{2d}u^2 = 0 \tag{3.12}$$

Simplifications

The following simplifications to modeling flow simulations are made in this project.

- Continuity equation disregarded since there are no changes in phase in the pipeline
- Energy equation disregarded since the system is well insulated and therefore adiabatic

That makes the momentum equation only equation left for simulating. In horizontal or near horizontal pipes with the stratified liquid flowing at the bottom and gas flowing above the momentum balance yield. (Speeding, 1996)

$$-A_f\left(\frac{dP}{dL}\right)_f - \tau_{wf}S_f + \tau_i S_i - \rho_f A_f g\sin\alpha \tag{3.13}$$

$$-A_g\left(\frac{dP}{dL}\right)_g - \tau_{wg}S_g + \tau_i S_i - \rho_g A_g g\sin\alpha \tag{3.14}$$

Where shear stresses τ_{wg} and τ_{wf} are the shear stresses causes by friction between the pipe wall and the two phases. τ_i is the friction between the two phases.

$$\tau_{wf} = f_f\frac{\rho_f V_f^2}{2} \tag{3.15}$$

$$\tau_{wg} = f_g\frac{\rho_g V_g^2}{2} \tag{3.16}$$

$$\tau_i = f_i\rho_G\frac{(V_g - V_f)^2}{2} \tag{3.17}$$

3.4 Void fraction

Many void fraction correlation exists but they are restricted in terms of handling different variety of data sets. It can be very hard to estimate the void fraction in two phase flow in pipelines, because of high temperature and large pipe size. Most simplest way of calculate the void fraction is the fraction between the area of steam and the total area of a given cross section of a pipe.

$$\alpha = \frac{A_g}{A_g + A_f} \tag{3.18}$$

The basic homogenous void fraction is as follows.

$$\alpha = \left[1 + \left(\frac{1-x}{x}\right)\left(\frac{\rho_g}{\rho_f}\right)S\right]^{-1} \tag{3.19}$$

Where S is slip ratio:

$$S = \frac{v_g}{v_f} \tag{3.20}$$

Where v is the velocity af the gas phase and v_f is the velocity of the liquid phase. In homogenous model it can be assumed that the gas and the liquid phase travel at the same pace giving $S = 1$. There are many other relations for the void fraction which extend the simple homogenous void fraction model by using different slip ratio. Zivi proposed the slip ratio to be dependent on the density ratio rather than velocity ratio. (Zivi, 1964)

$$S = \left(\frac{\rho_f}{\rho_g}\right)^{1/3} \tag{3.21}$$

Modified homogenous model by Zivi looks like

$$\alpha = \left[1 + \left(\frac{1-x}{x}\right)\left(\frac{\rho_g}{\rho_f}\right)^{2/3}\right]^{-1} \tag{3.22}$$

Chisholm also made a correlation for the slip ratio (Chisholm, 1973)

$$S = \left(\frac{\rho_f}{\rho_m}\right)^{1/2} \tag{3.23}$$

Where ρ_m is

$$\rho_m = \left(\frac{x}{\rho_g} + \frac{1-x}{\rho_f}\right)^{-1} \tag{3.24}$$

Which makes the homogenous model look like

$$\alpha = \left[1 + \left(\frac{1-x}{x}\right)\left(\frac{\rho_g}{\rho_f}\right)\left(1 + x\left(\frac{\rho_f}{\rho_g} - 1\right)\right)^{1/2}\right]^{-1} \tag{3.25}$$

Many other models have been made to determine the void fraction. In table 3.1 few void fraction correlation are listed.

Author (Butterworth, 1974)	Void fraction correlation	
Lockhart-Martinelli model (1949)	$\alpha = \left[1 + 0.28\left(\frac{1-x}{x}\right)^{0.64}\left(\frac{\rho_g}{\rho_f}\right)^{0.36}\left(\frac{\mu_f}{\mu_g}\right)^{0.07}\right]^{-1}$	(3.26)
Turner and Wallis model (1965)	$\alpha = \left[1 + \left(\frac{1-x}{x}\right)^{0.72}\left(\frac{\rho_g}{\rho_f}\right)^{0.4}\left(\frac{\mu_f}{\mu_g}\right)^{0.08}\right]^{-1}$	(3.27)
Thome model (1964)	$\alpha = \left[1 + \left(\frac{1-x}{x}\right)\left(\frac{\rho_g}{\rho_f}\right)^{0.89}\left(\frac{\mu_f}{\mu_g}\right)^{0.18}\right]^{-1}$	(3.28)
Baroczy model (1966)	$\alpha = \left[1 + \left(\frac{1-x}{x}\right)^{0.74}\left(\frac{\rho_g}{\rho_f}\right)^{0.65}\left(\frac{\mu_f}{\mu_g}\right)^{0.13}\right]^{-1}$	(3.29)
Smith model (1969)	$\alpha = \frac{x}{\rho_g}\left[\left[1 + 0.12(1-x)\right]\left[\frac{x}{\rho_g} + \frac{1-x}{\rho_f}\right] + \frac{(1.18(1-x))(g\sigma(\rho_f-\rho_g))^{0.25}}{G\rho_f^{0.5}}\right]^{-1}$	(3.30)

Table 3.1: Void fraction

3.5 Friction factor

Friction factor is a dimensionless coefficient. It can be found by a Moody diagram 3.1 or by calculating it. Calculations for friction factor are used from the liquid single phase as a reference.
The list below is the most used equation calculating the friction factor. (Kiijarvi, 2011)

- Blasius
- Colebrook-White (1939)
- Swamee-Jain
- Haaland (1984)
- Serghides (1984)
- Goudar–Sonnad

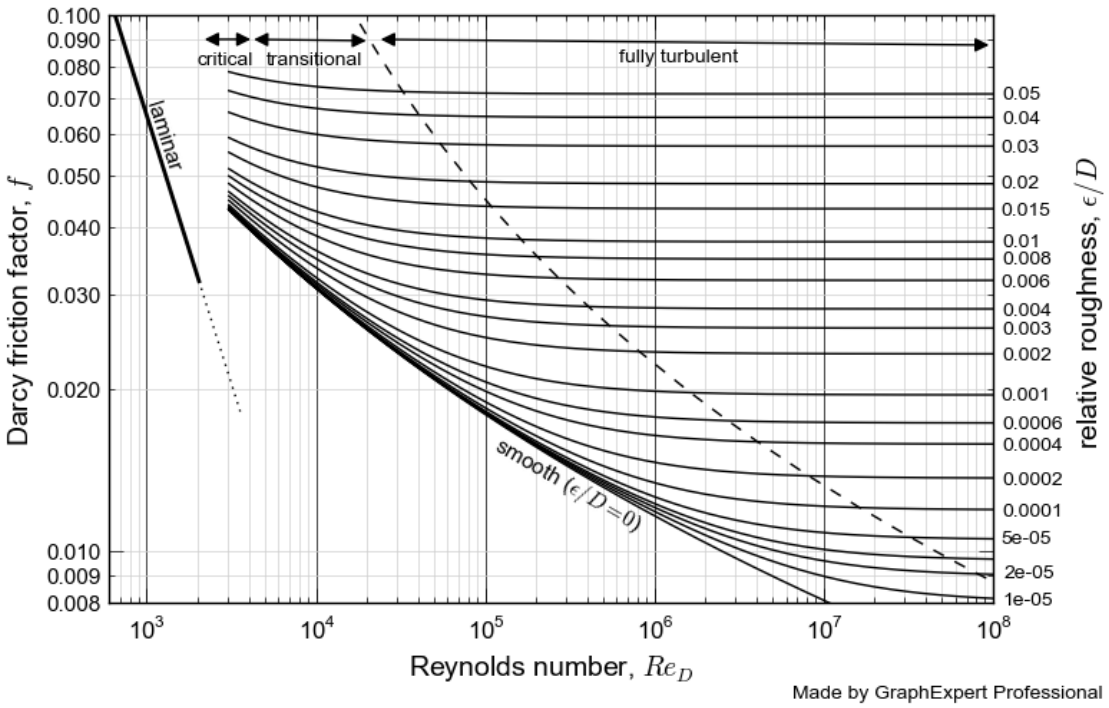

Figure 3.1: Moody Diagram

Blasius

The most simple equation for Darcy friction factor is the Blasius equation. It can only be applied to smooth pipes since the equation doesn't takes pipe roughness into the calculations.

$$f = \frac{0.316}{Re^{0.25}} \tag{3.31}$$

Colebrook-White

The Colebrook-White, was developed in 1939, combines experimental results from turbulent flow in smooth and rough pipes. Iteration is needed to determine the friction factor, often only a few iterations are needed. Colebrook-White equation is mostly used and the following equations 3.33 - 3.36 are variations from the Colebrook-White equations.

$$\frac{1}{\sqrt{f}} = -2\log_{10}\left(\frac{\epsilon}{3.7D}\frac{2.51}{Re\sqrt{f}}\right) \tag{3.32}$$

Where Re is the Reynolds number

$$Re = \frac{D\rho_f v}{\mu_f}$$

Where D is the pipe diameter and μ_f is the dynamic viscosity of the fluid.

Swamee-Jain

Swamee-Jain equation can be used on rough pipes to solve for the Darcy–Weisbach friction factor with no iteration.

$$f = 0.25\left[\log_{10}\left(\frac{\epsilon}{3.7D} + \frac{5.74}{Re^{0.9}}\right)\right]^{-2} \tag{3.33}$$

Haaland

The Haaland equation was developed by a Norwegian Institute of Technology professor Haaland in 1984. In Haaland equation no iteration is needed like Swamee-Jain

equation 3.33.

$$f = \left[-1.8 \log_{10} \left[\left(\frac{\epsilon}{3.7} \right)^{1.11} + \frac{6.9}{Re} \right] \right]^{-2} \tag{3.34}$$

Serghides

Serghides equation was developed in 1984.

$$f = \left[A - log_{10} \left(\frac{(B-A)^2}{C - 2B + A} \right] \right]^{-2} \tag{3.35}$$

Where

$$A = -2 \log_{10} \left(\frac{\epsilon}{3.7D} + \frac{12}{Re} \right)$$

$$B = -2 \log_{10} \left(\frac{\epsilon}{3.7D} + \frac{2.51A}{Re} \right)$$

$$C = -2 \log_{10} \left(\frac{\epsilon}{3.7D} + \frac{2.51B}{Re} \right)$$

Goudar–Sonnad

Goudar–Sonnad found his own friction factor.

$$f = \left[\frac{1}{a \times \left[\ln(\frac{d}{q}) + D_{CFA} \right]} \right]^2 \tag{3.36}$$

Where

$$a = \frac{2}{\ln(10)} \quad , b = \frac{e/D}{3.7} \quad , d = \frac{\ln(10) \times Re}{5.02} \quad \text{and } s = b \times d + \ln(d)$$

$$q = s^{(s/s+1)} \quad , g = b \times d + \ln \frac{d}{q} \quad , z = \ln \frac{q}{g} \quad \text{and } D_{LA} = z \times \frac{g}{g+1}$$

$$D_{CFA} = D_{LA} \times \left[1 + \frac{z/2}{(g+1)^2 + (z/3) \times (2g-1)} \right]$$

3.6 Friction correction factor

The standard approach to correlating two-phase frictional losses is to assume the total system mass flow rate is saturated liquid and then multiply by an empirical correction factor Φ. There are many ways to determine the friction correction factor. 9 models were compared to the measured data. 2 pressure dependant and 7 mass flux dependant.

- Becker
- Martinelli and Nelson (1948)
- Friedel (1979)
- Beattie (1949)
- Lockhart and Martinelli (1949)
- Baroczy (1966)
- Wallis (1969)
- Churchill (1973)
- Grönnurud (1972)

3.6.1 Pressure dependent correction factor

Becker

Beckers is a very simple way to define the friction correction factor.(Pálsson, 2009)

$$\Phi^2 = 1 + 2400\left(\frac{x}{p}\right)^{0.96} \tag{3.37}$$

Where p is liquid pressure and x is the quality of the steam.

Martinelli and Nelson

Martinelli and Nelson made a graph for the value of Φ^2 as a function of x and p. This graph has ben derived into the following equations. The model gives the best result when $\mu_f/\mu_g > 1000$ and $G > 100kg/m^2s$ (mass flux).

$$log_{10}(\Phi^2) = F(p)G(x) \tag{3.38}$$

$$F(p) = \begin{Bmatrix} 1.257 - 1.053(p/p_c)^{0.261} \text{ ef } p/p_c < 0.5 \\ 0.621(1 - p/p_c)^{0.715} \text{ ef } p/p_c > 0.5 \end{Bmatrix}$$

$$G(x) = \begin{Bmatrix} 3x^{0.2} \text{ ef } x < 0.8 \\ 2.869(1 - 1.154(x - 0.8)^2) \text{ ef } x > 0.8 \end{Bmatrix}$$

Where p_c is the critical pressure at 221.2 bar.(Hewitt, 1982; Þorbjörn Karlsson, 1979)

3.6.2 Mass flux dependent correction factor

Friedel

Friedel gathered 25.000 data points and developed his multiplier to these points. His experiments were done in a small diameter pipes. It shows good results in predicting two-phase frictional multiplier for smooth pipes with $D > 7mm$ and $\mu_f/\mu_g \ll 1000$.(Awad & Muzychka, 2004)

$$\Phi^2 = E + \frac{3.24FH}{Fr^{0.045}We^{0.035}} \tag{3.39}$$

Where

$$E = (1-x)^2 + x^2\frac{\rho_f}{\rho_g}\frac{f_f}{f_g} \tag{3.40}$$

$$F = x^{0.78}(1-x^2)^{0.24} \tag{3.41}$$

$$H = \left(\frac{\rho_f}{\rho_g}\right)^{0.91}\left(\frac{\nu_g}{\nu_f}\right)^{0.19}\left(1-\frac{\rho_g}{\rho_f}\right)^{0.7} \tag{3.42}$$

Froude number

$$Fr = \left(\frac{\dot{m}}{A}\right)^2\frac{1}{gD\rho_m^2} \tag{3.43}$$

Weber number

$$We = \left(\frac{\dot{m}}{A}\right)^2\frac{D}{\sigma\rho_m^2} \tag{3.44}$$

The parameter σ is the surface tension of water and can be calculated as follows

$$\sigma = 0.2358\left(1-\tfrac{T}{T_c}\right)^{1.256}\left(1-0.625\left(1-\tfrac{T}{T_c}\right)\right) \tag{3.45}$$

Mean density

$$\rho_m = \left(\frac{x}{\rho_g} + \frac{1-x}{\rho_f}\right)^{-1} \tag{3.46}$$

Where ρ_g and ρ_f is found with a Matlab code XSteam which uses water and steam properties according to IAPWS IF-97. The temperature to calculate the density is $190°C$ (Holmgren, 2010)

Beattie

Beattie correlation is defined in a simpler manner:

$$\Phi^2 = \left(1+x\left(\frac{\rho_f}{\rho_g}-1\right)\right)^{0.8}\left(1+x\left(\frac{3.5\mu_g+2\mu_f}{(\mu_g+\mu_f)\rho_g}-1\right)\right)^{0.2} \tag{3.47}$$

Lockhart and Martinelli model

The Lockhart and Martinelli model is the most widely used correlation in the history of two phase flow frictional calculations(Awad & Muzychka, 2004).

$$\Phi^2 = 1 + \frac{C}{X} + \frac{1}{X^2} \tag{3.48}$$

Where $C = 20$ if both phases are turbulent, $C = 12$ if only the gas is turbulent, $C = 10$ if only the liquid is turbulent and $C = 5$ if both are laminar. They defined a parameter X^2 as the ratio between the frictional pressure gradient for the liquid phase flowing alone in a smooth pipe against the gas phase flowing alone, or

$$X^2 = \frac{(dp/dz)_f}{(dp/dz)_g} \tag{3.49}$$

Where

$$\left(\frac{dp}{dz}\right)_g = \frac{2f_g G^2 x^2}{D\rho_g} \tag{3.50}$$

and

$$\left(\frac{dp}{dz}\right)_f = \frac{2f_f G^2 (1-x)^2}{D\rho_f} \tag{3.51}$$

Where G is mass flux $[Kg/m^2 s]$. The biggest advantage of the Lockhart Martinelli model is that it can be used for all flow patterns (Awad and Muzychka (2004)) however a relatively low accuracy must be accepted in return. This method has a large prediction error and the Friedel separate flow model should preferably be used (Hewitt et al. (1982)).

Baroczy model

$$\Phi^2 = 1 + (\Gamma^2 - 1)(B_R x^{(2-n)/2}(1-x)^{(2-n)/2} + x^{2-n}) \tag{3.52}$$

Where B_R is the Baroczy correlation for rough pipes. Chisholm studied the influence of pipe surface roughness on friction pressure gradient during two phase flow. B_S for smooth pipes and B_R for rough pipes.(Awad & Muzychka, 2004).
Where

$$\Gamma = \left(\frac{(dp/dz)_g}{(dp/dz)_f}\right)^{0.5} \tag{3.53}$$

$$B_R = B_S \left[0.5 \left(1 + \left(\frac{\mu_g}{\mu_f} \right)^2 + 10^{-600\epsilon/d} \right) \right]^{\frac{0.25-n}{0.25}} \tag{3.54}$$

Γ	$G(kg/m^2s)$	B_S
$0 < \Gamma \leq 9.5$	$G \leq 500$	4.8
	$500 < G < 1900$	$240/G$
	$G \geq 1900$	$55G^{1/2}$
$9.5 < \Gamma < 28$	$G \leq 600$	$520/\Gamma G^{1/2}$
	$G > 600$	$21/\Gamma$
$\Gamma \leq 28$		$15000/\Gamma^2 G^{1/2}$

Table 3.2: Baroczy Values for smooth pipes

Where G is

$$G = \frac{\dot{Q}_t}{A} \tag{3.55}$$

Wallis

Wallis assumed that the flow in the smooth pipes were turbulent with Fanning friction factor empirically by the Blasius equation $n = 0.25$.(Awad & Muzychka, 2004) The correlation is:

$$\Phi^2 = \left(1 + x\frac{\rho_f - \rho_g}{\rho_g} \right) \left(1 + x\frac{\mu_f - \mu_g}{\mu_g} \right)^{-1/4} \tag{3.56}$$

The correlation multiplier can be evaluated for any steam quality (x), temperature and pressure condition assuming that density and viscosity data area available. This method works quite well for dispersed phase flow but has tendency to under predict the pressure drop for separated flow.

Churchill

Chuchill model was developed to take the effect of the mass flux (G) on Φ^2 into account. Chuchill's correlation spanned the entire range of laminar, transition and turbulent flow in pipes.(Awad & Muzychka, 2004)

$$\Phi^2 = \left(\frac{f_m}{f_{lo}} \right) \left(1 + x\frac{\rho_l - \rho_g}{\rho_g} \right) \tag{3.57}$$

Where

$$f_m = 2\left[\left(\frac{8}{Re_m}\right)^{12} + \frac{1}{(a_m + b_m)^{3/2}}\right]^{1/12} \tag{3.58}$$

$$a_m = \left[2.457ln\frac{1}{(7/Re_m)^{0.9} + (0.27\epsilon/d)}\right] \tag{3.59}$$

$$b_m = \left(\frac{37530}{Re_m}\right)^{16} \tag{3.60}$$

$$f_{lo} = 2\left[\left(\frac{8}{Re_{lo}}\right)^{12} + \frac{1}{(a_{lo} + b_{lo})^{3/2}}\right]^{1/12} \tag{3.61}$$

$$a_{lo} = \left[2.457ln\frac{1}{(7/Re_{lo})^{0.9} + (0.27\epsilon/d)}\right] \tag{3.62}$$

$$b_{lo} = \left(\frac{37530}{Re_{lo}}\right)^{16} \tag{3.63}$$

Where the Reynolds number are as follows.

$$Re_m = \frac{Gd}{\mu_m} \tag{3.64}$$

$$Re_{lo} = \frac{Gd}{\mu_f} \tag{3.65}$$

The subscript $_{lo}$ stands for liquid only.

Grönnurud

Grönnurud developed a two phase multiplier in 1972.

$$\Phi^2 = 1 + \left(\frac{dp}{dz}\right)_{Fr}\left[\frac{\left(\frac{\rho_f}{\rho_g}\right)}{\left(\frac{\mu_f}{\mu_g}\right)^{0.25}} - 1\right] \tag{3.66}$$

Where the frictional pressure gradient depends on the Froude number and is.

$$\left(\frac{dp}{dz}\right)_{Fr} = f_{Fr}[x + 4(x^{1.8} - x^{10} f_{Fr}^{0.5})] \tag{3.67}$$

If $Fr_L > 1$ then the friction factor $f_F r = 1$, else if $Fr_L < 1$ then

$$f_{Fr} = Fr_L^{0.3} + 0.0055\left[ln\frac{1}{Fr_L}\right]^2 \tag{3.68}$$

Where Fr_L is the Froude number for liquid phase

$$Fr_L = \frac{\dot{m}_{total}^2}{gD_i\rho_L^2} \tag{3.69}$$

3.7 Friction correction factor for bends

Similar to straight pipe, correction friction factor is needed to correlate two phase frictional pressure loss in in bends and other fittings. Four correction factor for 90° bends will be examined in this chapter.(Azzi, Friedel, & Beladi, 2000) Figure 3.2 shows the parameters of a bend.

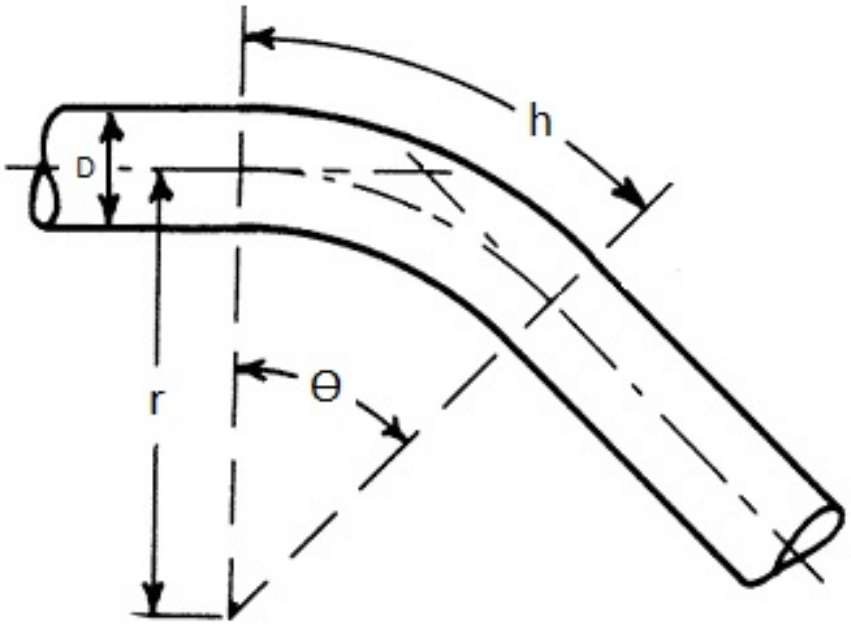

Figure 3.2: Pipe bend

Chisholm B-type

Chisholm suggested two phase multiplier. First in 1980, equation 3.70.

$$\Phi^2 = 1 + \left(\frac{\rho_f}{\rho_g} - 1\right)(Bx(1-x) + x^2) \tag{3.70}$$

And in 2000 he made changes to his early equation.

$$\Phi^2 = \frac{1}{(1-x)^2}(1 + \left(\frac{\rho_f}{\rho_g} - 1\right)(Bx(1-x) + x^2)) \tag{3.71}$$

- B = $1 + 2.2/(K(2 + r/D_{in}))$
- K = 1.6 fh

Where f is the friction factor, and h is the length of the bend, see figure 3.2. Since there are 5 models for friction factor in rough pipes, an average value of the 5 models is used.

Chisholm C-type (1987)

Chisholm suggested another multiplier, C-type, in 1967.

$$\Phi^2 = 1 + \frac{C}{X} + \frac{1}{X^2} \tag{3.72}$$

$$C = \left(1 + 25\frac{D}{h}\right)\left(\left(\frac{\rho_f}{\rho_g}\right)^{0.5} + \left(\frac{\rho_g}{\rho_f}\right)^{0.5}\right) \tag{3.73}$$

$$X = \left(\frac{1-x}{x}\right)^{0.9}\left(\frac{\mu_f}{\mu_g}\right)^{0.1}\left(\frac{\rho_g}{\rho_f}\right)^{0.5} \tag{3.74}$$

P. Sookprasong

P. Sookprasong made his edition of the multiplier

$$\Phi^2 = \frac{(\rho_f u_f + \rho_g u_g)(u_g + u_f)}{\rho_l u_l^2} \tag{3.75}$$

4 Pressure changes

Change in pressure in gas or liquid through a system, is very important variable when designing gathering pipelines in geothermal power plants. The pressure and steam quantity decides the power output of the turbine. That is why, when designing pipelines in a geothermal power plant minimizing the total pressure change and by reducing the number of bends and other fittings on the pipeline is key in designing the pipe route. Since the quantity of the steam flowing into the system varies the pressure in the steam pipes is controlled by opening a control valve, thus releasing the steam through a hood. This ensures that the same pressure in all the gathering pipes is the same entering the turbine.

Pressure change in two phase flow calculations are derivatives and uses the basic rules for mass, momentum and energy.

- Pressure changes caused by gravity (height changes in the pipeline)
- Pressure changes caused by momentum
- Pressure changes caused by friction

The following simplifications have be applied to the calculations.

- The pressure stays the same throughout the cross section of the pipe
- The velocity of the steam and or the liquid stays the same through all the pipeline, though the velocity can vary between the phases.
- The flow is isothermal and adiabatic since the pipelines are insulated and the pressure drop is minimal against the total pressure in system

4.1 Pressure changes from height difference

Pressure change from height difference in two phase flow can be calculated by 4.1

$$\Delta P_H = g \int_0^H \rho_m sin\Theta dz \tag{4.1}$$

Where $\rho_m = \alpha\rho_g + (1-\alpha)\rho_f$. To be able to calculate the pressure change from height difference, void fraction must be established. Which is the ratio between cross section area of steam in the pipe against the total cross section area in the pipe. See chapter 3.4

4.2 Pressure changes caused by momentum changes

Momentum in two phase flow can be calculated by 4.2

$$\dot{M} = \dot{m}_g u_g + \dot{m}_f u_f = (x u_g + (1-x)\, u_f)\dot{m} \tag{4.2}$$

By knowing the velocity of each phase as shown in 4.3 and 4.4

$$u_g = \frac{\dot{m}_g}{\rho_g A_g} = \frac{x}{\rho_g \alpha}\frac{\dot{m}}{A} \tag{4.3}$$

$$u_f = \frac{\dot{m}_f}{\rho_f A_f} = \frac{(1-\alpha)}{\rho_f (1-\alpha)}\frac{\dot{m}}{A} \tag{4.4}$$

The 4.2 becomes

$$\dot{M} = \Big(\frac{x^2}{\rho_g \alpha} + \frac{(1-x)^2}{\rho_f (1-\alpha)}\Big)\frac{\dot{m}^2}{A} \tag{4.5}$$

Then the total force on a pipe cross section can be written as

$$F = \rho A + \dot{M} \tag{4.6}$$

But assumptions state that the characteristics of the medium stays the same from the borehole to the separation station, pressure drop caused by momentum (acceleration) can be ignored.

$$h_M = 0 \tag{4.7}$$

4.3 Pressure changes caused by friction

Friction pressure change in steady pipe flow is calculated using the Darcy-Weisbach equation. This equation includes the Darcy friction factor.(Kiijarvi, 2011)

$$h_f = \frac{fL}{D}\frac{u^2}{2g} \tag{4.8}$$

Equation 4.8 is pressure head in meters. For a pipe of length L the change in pressure can be written as follows.

$$\Delta P_f = \frac{f\rho L}{D}\frac{u^2}{2} \tag{4.9}$$

Where f, D and u represent, respectively the Darcy friction factor, pipe inner diameter and liquid velocity. The Darcy friction factor was discussed in section 3.5

The pressure drop by friction is then

$$\Delta P_f^{twophase} = \Phi^2 \Delta P_f^{singlephase} \tag{4.10}$$

Where Φ is friction correction factor which was introduced in section 3.6

4.3.1 Pressure drop through different installations

Pressure drop in a pipeline with junctions, bends, expansion units and valves can be calculated using a number of equations. Three of them will be discussed in this

chapter.

Chisholm

Chisholm presented a pressure drop equation in bends, see equation 4.11.(Chisholm, 1983)

$$\Delta P_{fi} = \Phi^2 K_{sp} \frac{G^2}{2\rho_f} \tag{4.11}$$

Where

$$K_{sp} = f_f \frac{h}{D_{in}} + 0.294 \left(\frac{r}{D_{in}} \right)^{0.5} \tag{4.12}$$

Where G is mass flux, r is radius of bend, h is the equal length of bend and D is the inner diameter of bend (see figure 3.2).

Darcy-Weisbach

It is also possible to use the Darcy-Weisbach equation 4.9 to calulate the pressure drop.

$$\Delta P_{fi} = \Phi^2 \frac{f \rho_m \overline{V}^2 h}{2D} \tag{4.13}$$

Where $\overline{V}$ average velocity of the equivalent single-phase flow and can be calculated in the following equation. (H.D. Zhao & Freeston, 2000)

$$\frac{\overline{V_f}}{\overline{V}} = \frac{(1-\sqrt{\alpha})^{8/7}\left(1+\frac{8}{7}\sqrt{\alpha}\right)}{(1-\alpha)} \tag{4.14}$$

Where $\overline{V_f}$ is the liquid phase velocity.

$$\overline{V_f} = 1.1(1-x)\frac{\dot{m}(1-x)}{\rho_f(1-\alpha)A} \tag{4.15}$$

Sreenivas Jayanti

Sreenivas Jayanti found out that both friction and momentum change cause pressure change in bends and can be summed up in two components. Change of direction

and roughness. (Jayanti, 2011)

$$\Delta P_{fi} = \Phi^2 \left(\frac{1}{2} f \rho_f u^2 \frac{\pi R_b}{D} \frac{\Theta}{180^\circ} + \frac{1}{2} k_b \rho u^2 \right) \tag{4.16}$$

Where Θ is the angle of the bend and k_b loss coefficient for single phase from figure 4.1.

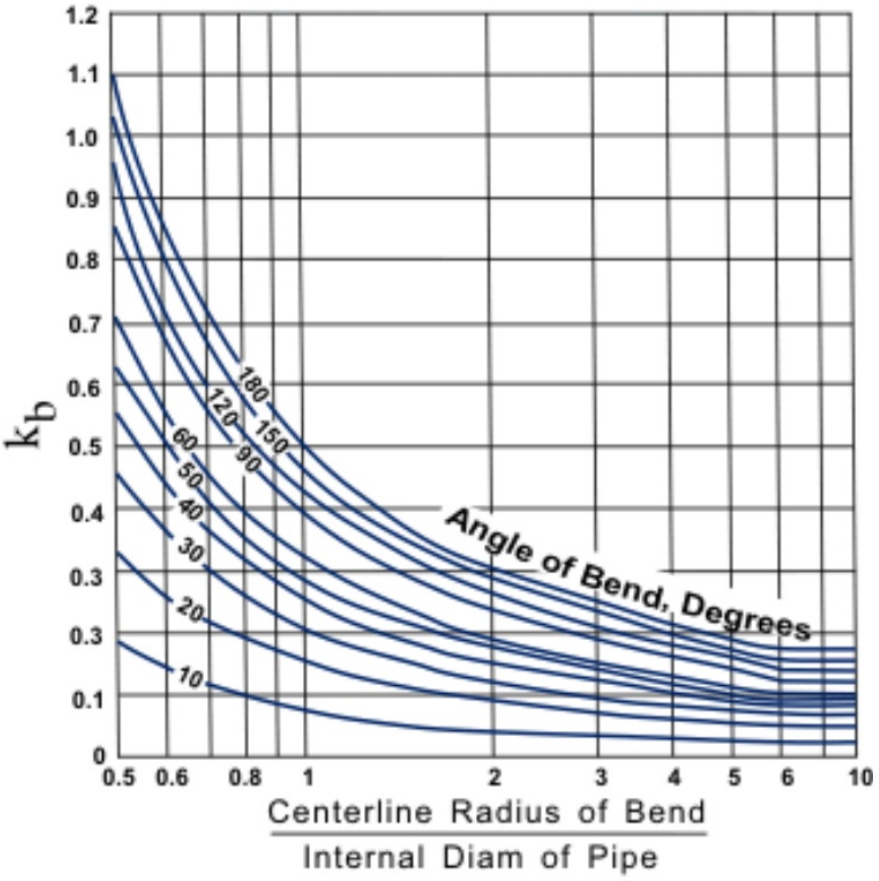

Figure 4.1: Bend loss coefficients for a pipe (Babcock & WilcoxCo, 1978)

Where Φ is friction correction factor which was introduced in section 3.7

4.4 Total Pressure changes

The total pressure change is then the sum of pressure drop from height, friction in straight pipes and in bends. Since there are 3 equations for calculating the pressure

drop in bends in this project, an average from these 3 will be used.

$$dP_{tot} = \Delta P_H + \Delta P_f + \Delta P_{fi} \tag{4.17}$$

5 Measurements

Measurements were made at Hellisheiði power plant at the upper region. A differential manometer meter was used.

5.1 Technique

Two measurements were made in every gathering pipeline. At the top near the borehole, after the control valve, and near the separation station. Since the pressure in the system is around 10 bar the conventional analog pressure meter is not accurate enough so a differential manometer was used. An insulated tank was used and pressurized. The difference manometer was a 1.5 bar manometer, so the difference in pressure between the gathering pipeline and the reference tank could not exceed 1,5 bar. With values of both measurements, at the top and at the separation station, a pressure difference can be made.
Figure 5.2 and 5.1 shows the measurement setup between the gathering pipeline and the differential manometer.

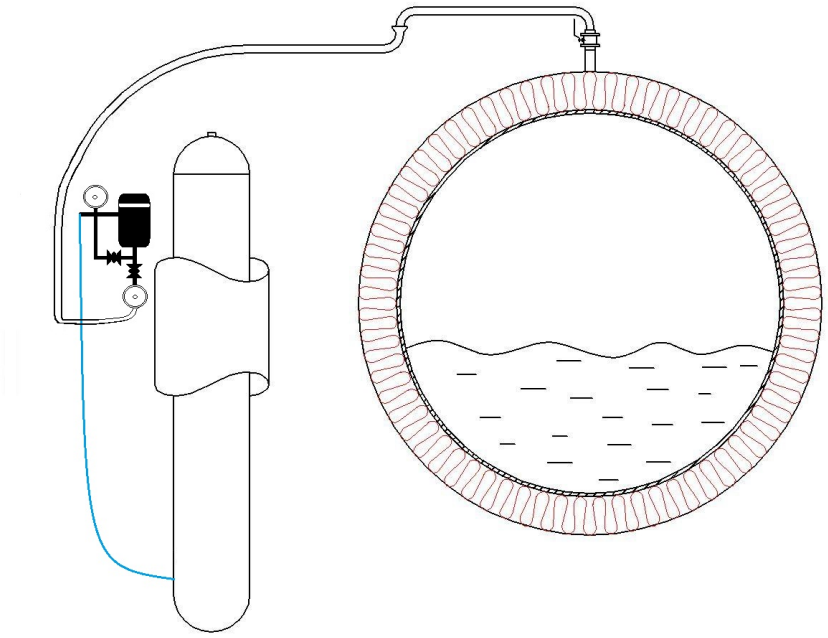

Figure 5.1: Schematic setup

Figure 5.2: Measurement setup

5.2 Equipment

The differential pressure meter consists of the following parts.

- Insulated tank
- 2x 20bar analog pressure meters
- 1x 1.5bar analog pressure meter
- Casing for the 2bar analog pressure meter
- 2x PN16 gas ball valves

A detailed view of the differential manometer can be seen in figure 5.3. Input 1 is where the gathering pipeline is connected to. Input 2 is the reference tank. Manometer 1 and 2 are a 20bar pressure gauge for input 1 and 2 respectively. Manometer 3 is the 1.5bar difference pressure meter. Accuracy in the equipment is dependent on the accuracy in the analog difference manometer. The accuracy of the manometer 3 is 0.05bar. The reference tank, a steel cylinder, $1200mm$ high and $200mm$ in diameter, which gives a volume of $0,038m^3$. The tank was insulated with 60mm rock wool, so the outside heat would not affect the pressure readings.

Calibration

Water column was used to calibrate the equipment. At atmospheric pressure of height of 10m of water is about 1 bar ($0.9806bar$). The calibration was done from 0m to 8m. Error in the differential manometer was $0.05bar$.

Problems with the equipment

There were a few problems with the equipment. A leak problem was discovered early on. The cause of the leak was the valves. They were ball valves dedicated for liquid phase use but not gas. They were exchanged for gas ball valves.

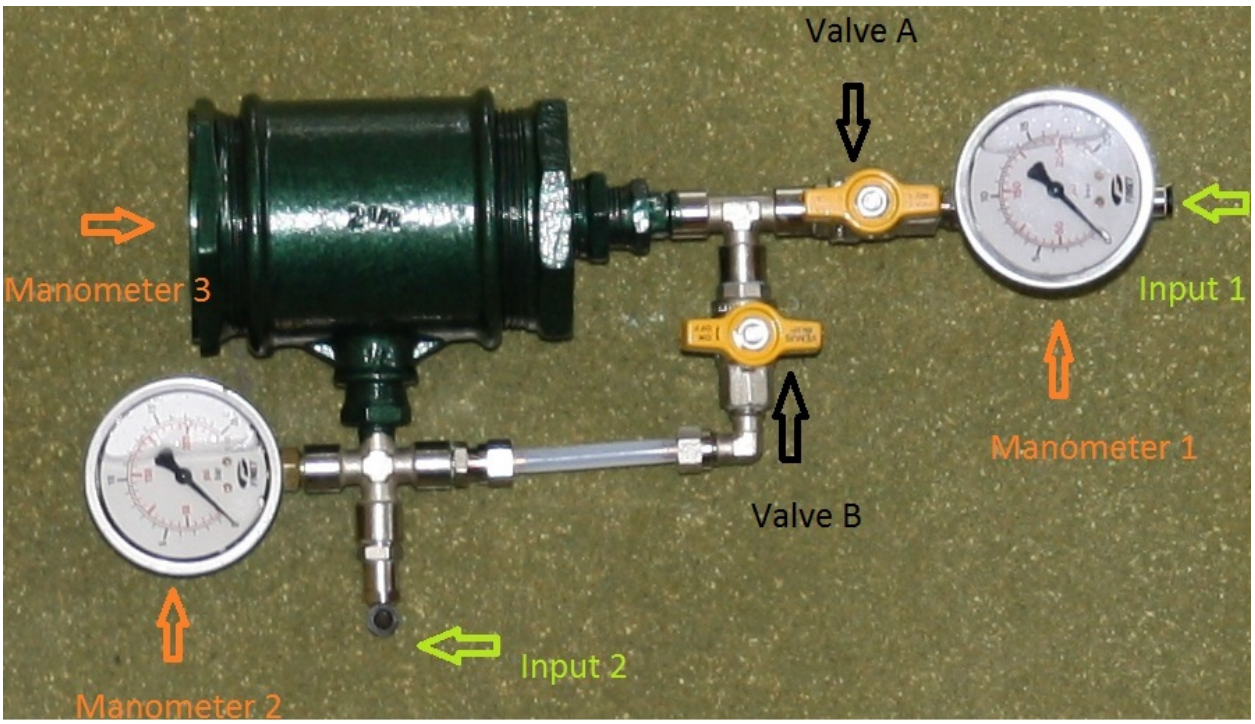

Figure 5.3: Differential manometer (Benjamin, 2013)

Early design

After many months of waiting for the digital pressure meters that were supposed to be used, the build of the pressure tank and calibration of the pressure meters was done. First when the project started, two digital pressure meters were to be used in the measurements. Measurements were to be done at both places, near the borehole and at the separation station, at the same time to be able to see the fluctuations in the system. Data from the digital pressure meters was collected with A/D alter and transformed the data to pressure value. A program in LabVIEW was made to analyze the measured data. Problem with the digital pressure meter was that they were very fragile. Use of the digital pressure meter was unsuccessful because the digital pressure meter was damaged in storage. Moist must have come in contact with the meter where it wasn't supposed to.

5.3 Measurements

Data for the gathering pipelines can be seen in Table 5.1 and 5.2.(Sigfússon & Kjartansson, 2013). The data was provided by Orkuveita Reykjavíkur.
Gathering pipelines consist of variable number of pipelines from boreholes which

merge into one. Measurements were made at one of the pipes before the merge and at the separation station, after the merge. In table 5.1 the borehole has been marked with a * signaling what pipe was measured. The enthalpy and the total mass flow is measured for the boreholes but the gas phase mass flow, gas and liquid velocity and the quality of steam are calculated with equations 3.6, 3.7 and 3.8 or 3.9 on page 7. The enthalpy for the gathering pipelines are in proportion to the mass flow in the boreholes, see equation 5.1. The collected data (Sigfússon & Kjartansson, 2013) has no information for the temperature of the medium or the roughness. That data was estimated at 192° and $1mm$.

Where the enthalpy for the gathering pipelines is calculated from the sum of enthalpy from the boreholes times the mass flow against the total mass flow in the gathering pipelines.

$$H_{total} = \frac{\sum H_i \times \dot{Q}_i}{\sum \dot{Q}_i} \tag{5.1}$$

Where $\dot{Q}_i$ and H_i are the mass flow and enthalpy respectively from the boreholes.

Table 5.2 shows the physical data of the gathering pipelines, such as the length and the height difference between the two measure points. These points are at the beginning of the gathering pipelines, before the gathering pipelines merge.

Overview of the upper region of Hellisheidi power plant can be seen in figure 5.4. Figures 5.5-5.8 shows in detail the measure points at the boreholes.

Holes and Pipelines	H [kj/kg]	$\dot{Q}_t$ [kg/s]	$\dot{m}_g$ [kg/s]	v_g [m/s]	v_f [m/s]	x
HE-6*	1950	29,4	16,6	10,4	0,078	0,56
HE-11	2180	50,8	34,8	23,2	0,097	0,68
HE-17	2050	65	39,8	24,3	0,153	0,61
Gathering pipeline 12*	2075	145	91,2	14,1	0,080	0,63
HE-7*	1450	76,7	22,7	13,1	0,33	0,30
HE-12	1750	67,9	31,1	19,5	0,22	0,46
HE-16	1120	27,2	3,9	2,65	0,14	0,14
Gathering pipeline 4*	1516	171,8	57,7	8,66	0,17	0,33
HE-4*	1100	49,5	7,0	5,2	0,25	0,14
HE-15	1900	35,1	18,1	8,4	0,11	0,52
HE-30	1900	42,3	23,0	15,8	0,12	0,54
Gathering pipeline 6*	2075	126,9	48,1	7,5	0,12	0,38
HE-47*	1600	101	38	5,5	0,09	0,38
Gathering pipeline 26	1600	101	38	5,5	0,09	0,38
HE-19*	2100	55,3	35,4	5,4	0,03	0,64
Gathering pipeline 16	2100	55,3	35,4	5,4	0,03	0,64
HE-50*	2306	16,9	12,6	8,07	0,03	0,75
HE-56	1500	56,7	18,9	12,6	0,23	0,33
HE-9	2660	9,2	8,5	4,2	0,004	0,93
HE-14	1200	31,7	6,4	5,5	0,15	0,20
HE-18	1400	42,8	12,3	10,8	0,18	0,30
HE-3	1372	25,9	7,2	5,3	0,11	0,28
HE-32	1470	47,7	15,2	10,1	0,20	0,32
HE-51	2770	5,0	4,9	2,2	0,0005	0,98
Gathering pipeline 3	1551	235,9	86,2	15,1	0,22	0,37

Table 5.1: Gathering pipeline data 1

Gathering pipeline	Length [m]	Height difference [m]	Bends	Tees
Gathering pipeline 12	1290	67,8	19	2
Gathering pipeline 4	671	38,1	9	0
Gathering pipeline 6	1016	53,3	10	0
Gathering pipeline 26	923	50,7	10	0
Gathering pipeline 16	999	53,4	11	0
Gathering pipeline 3	1233	44,7	19	2

Table 5.2: Gathering pipeline data 2

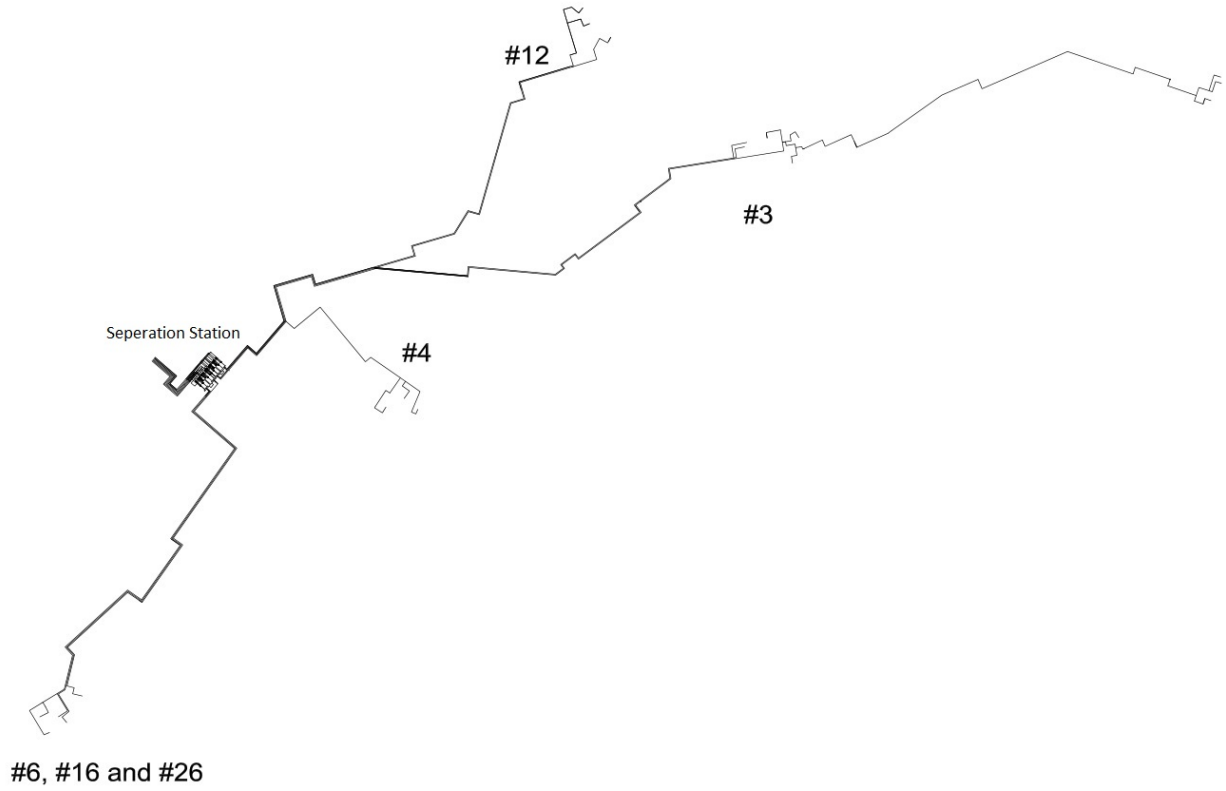

Figure 5.4: Hellisheidi, upper region, Overview

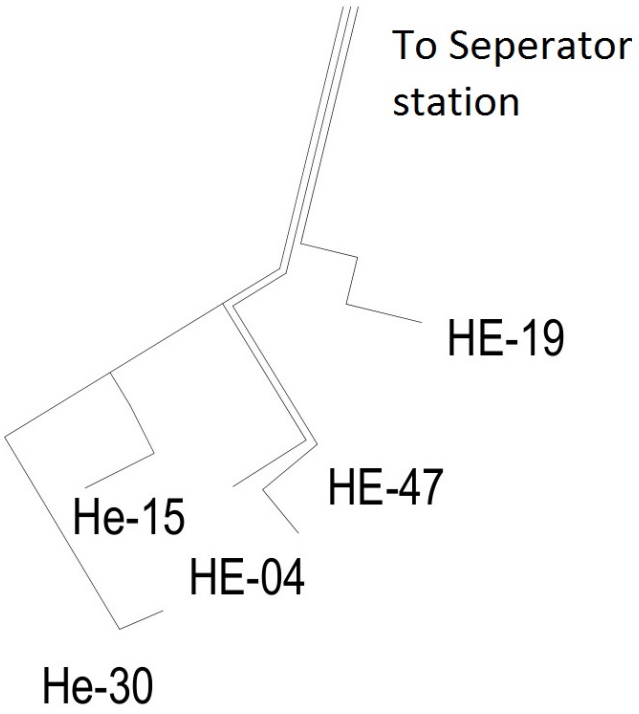

Figure 5.5: Gathering pipelines 6,16 and 26

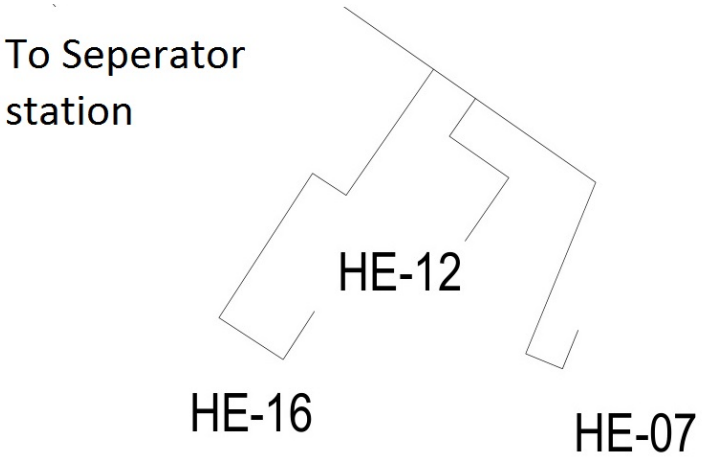

Figure 5.6: Gathering pipelines 4

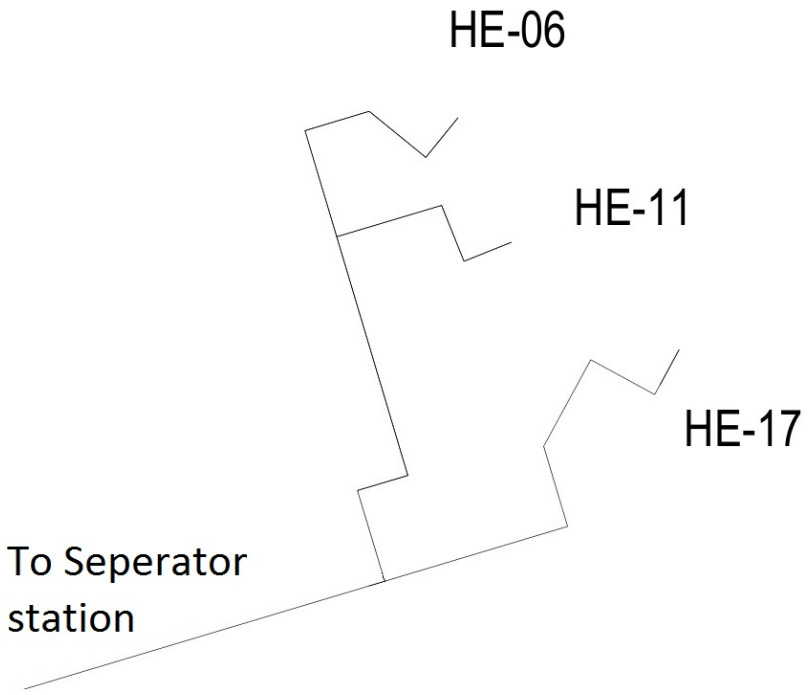

Figure 5.7: Gathering pipelines 12

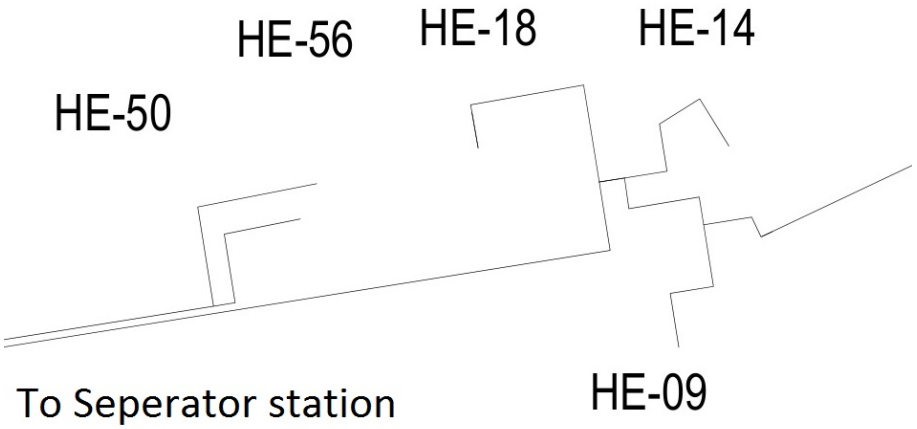

Figure 5.8: Gathering pipelines 3

6 Results

The following chapter shows the measured and compared to different sets of models of void fraction, friction factor and friction correction factor. The absolute error and spread of calculated data is compared to measurements. What changes in roughness does to the pressure prop is looked at and plotted. The collected data (Sigfússon & Kjartansson, 2013) has no information for the temperature of the medium nor the roughness. The calculations in the following chapter assume the temperature and the roughness at $190°C$ and $3mm$ respectively. In the pressure dependent model the pressure selected for the calculations for the friction correction factor is $9.5bar$ which is the average value of measured pressure in the gathering pipeline.

6.1 Comparison of Void fraction

In table 6.1 void fractions models, from section section 3.5 page 9, are displayed. Also the average value is calculated. It can be seen that the void fraction is very high. Which matches to value of gas and fluid velocity from table 5.1 on page 34.

	Gathering Pipelines					
Models	12	4	6	26	16	3
Homogenous	0.99	0.98	0.98	0.98	0.99	0.99
Zivi	0.97	0.92	0.93	0.93	0.99	0.93
Lockhart-Martinelli	0.96	0.93	0.93	0.93	0.98	0.94
Turner and Willis	0.91	0.80	0.82	0.82	0.91	0.82
Thom	0.99	0.97	0.98	0.97	0.99	0.98
Barozcy	0.97	0.93	0.94	0.93	0.97	0.94
Smith	0.97	0.91	0.93	0.92	0.97	0.93
Chisholm	0.96	0.90	0.91	0.91	0.96	0.91
Average	0.97	0.92	0.93	0.93	0.97	0.94

Table 6.1: Void fraction comparison

In figure 6.1 is a comparison of the void fraction named here above with increasing steam quality, an average value from gathering pipeline is used. It can be seen that

the void fraction increases very fast with increasing steam quality. The homogenous and Thom model are slightly quicker to reach steam quality of 1. Turner and Wallis model is the only one that is different than the other models. It gives much lower void fraction than other models. Mass quality is the steam quality.

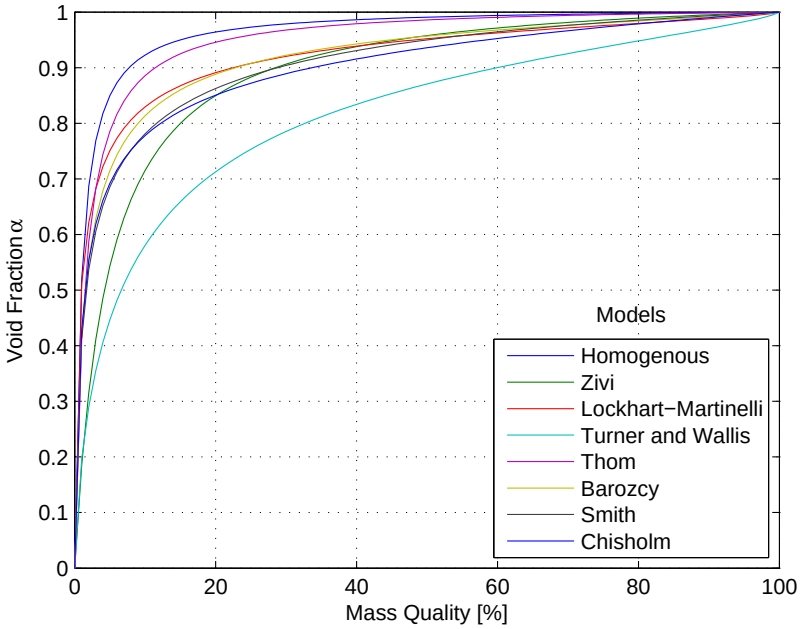

Figure 6.1: Comparison of Void fraction models

6.2 Comparison of friction factor

In table 6.2 the friction factor or the gathering pipelines is displayed. The friction factor is roughness dependent and in table 6.2 the roughness is 3mm. All but the Blasius equation shows similar results, because the Blasius equation is not roughness dependent.

	Gathering Pipelines					
Models	12	4	6	26	16	3
Colebrook	0.0196	0.0196	0.0196	0.0196	0.0198	0.0196
Swamee-Jain	0.0197	0.0196	0.0196	0.0197	0.0198	0.0196
Haaland	0.0197	0.0196	0.0196	0.0197	0.0198	0.0196
Blasius	0.0069	0.0057	0.0063	0.0066	0.0089	0.0054
Serghides	0.0197	0.0197	0.0197	0.0197	0.0200	0.0196
Goudar	0.0196	0.0196	0.0196	0.0196	0.0198	0.0196

Table 6.2: Friction factor comparison

6.3 Pressure drop models

As stated in chapter 3.5 there are pressure dependent models, mass flux dependent models and bend models in calculating the friction correction factor, Φ. In this chapter they will be examined with according to changing steam quality.
An average value from the gathering pipelines are used in figures 6.2, 6.3, 6.4 and 6.5 to show the changes in friction correction factors for the models.

6.3.1 Pressure dependent models

In figure 6.2 Becker model is plotted with different pressure, from 1 bar to 15 bar. The higher the pressure, the lower the change of friction correction factor with increasing steam quality becomes.
In figure 6.3 the friction correction factor increases until the steam quality reaches 0.8 then it decreases. Same as in the Becker model the higher the pressure, the lower the change of friction correction factor with increasing steam quality becomes.

6.3.2 Mass flux dependent models

Figure 6.4 shows comparison of Friedel, Beattie, Lockhart and Martinelly, Barozcy, Wallis, Churchill and Grönnerud friction correction factors with changing steam quality. All the models have the same tendency to increase with higher steam quality, except Grönnerud model. In Grönnerud model the correction factor decreases when the steam quality exceeds 0.8.

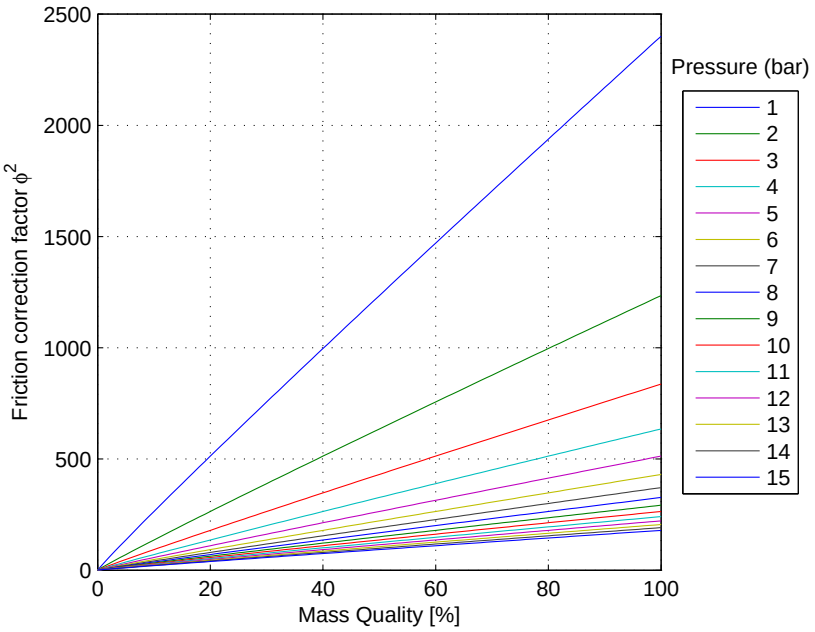

Figure 6.2: Becker model

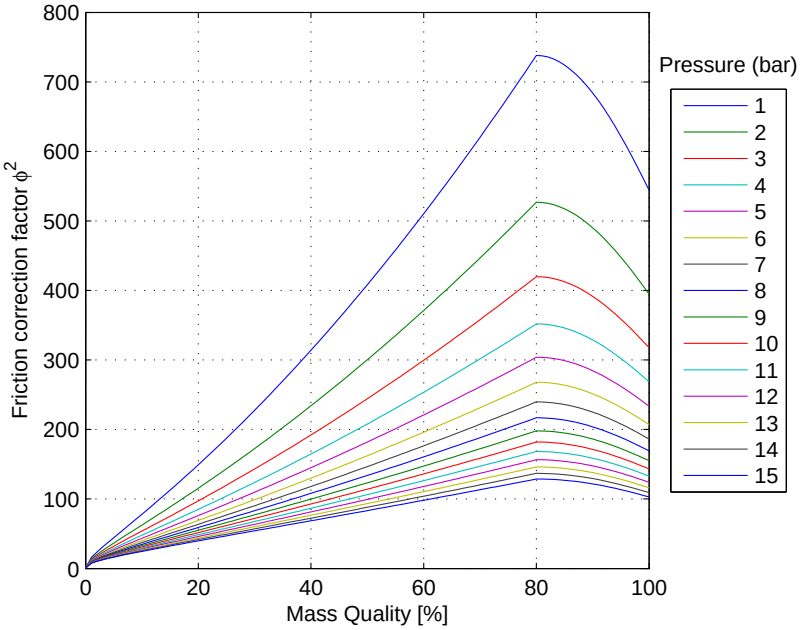

Figure 6.3: Martinelli and Nelsons model

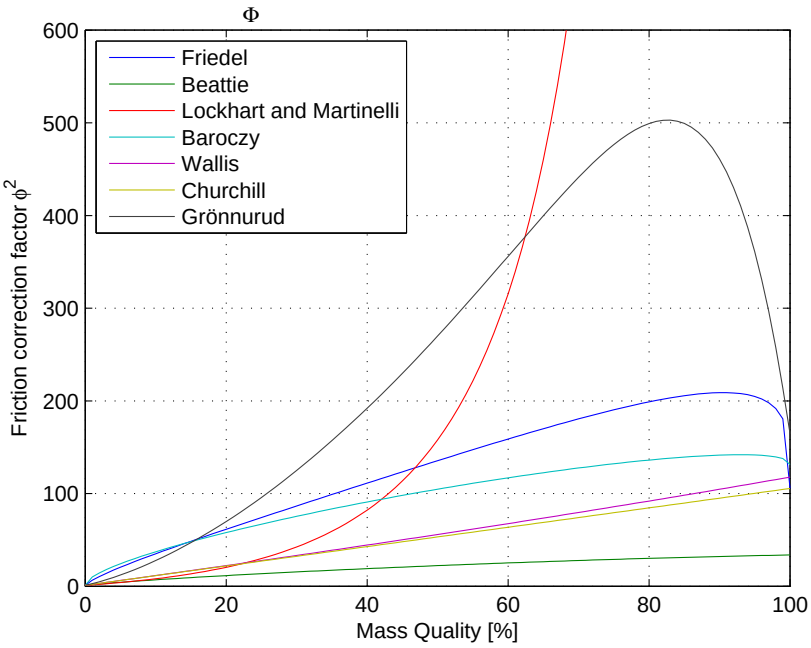

Figure 6.4: Comparison of friction correction factor

6.3.3 Bend models

Figure 6.5 shows comparison of correction factors for bends with changing steam quality. When the steam quality reaches over 50% the Chisholm type b (2000) and P.Sookprasong models increase very fast and give misleading result. The remaining two models give more realistic result across the range.

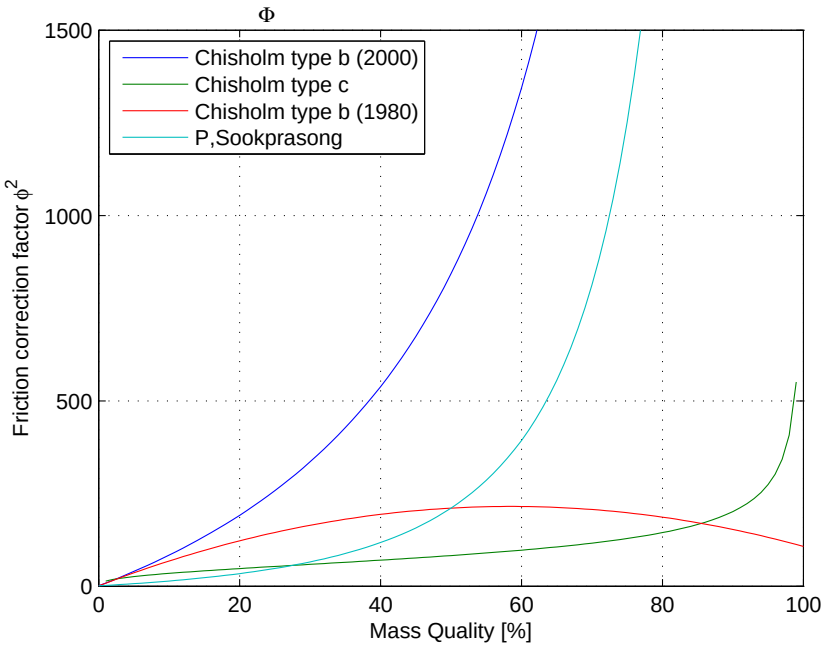

Figure 6.5: Comparison of friction correction factor for bends

6.4 Pressure drop

In this chapter pressure drop from gravity, friction in straight pipes and in bends will be examined and compared to the measured data.

Measured pressure drop

Table 6.3 shows the measured pressure drop in the gathering pipelines using the method described in chapter 5.

	Gathering Pipelines					
	12 [mbar]	4 [mbar]	6 [mbar]	26 [mbar]	16 [mbar]	3 [mbar]
Measured pressure drop	310	200	200	210	150	530

Table 6.3: Measured pressure drop

Pressure drop from gravity

Table 6.4 shows the predicted pressure drop in the gathering pipelines from height difference, from chapter 4.1.

	Gathering Pipelines					
	12 [mbar]	4 [mbar]	6 [mbar]	26 [mbar]	16 [mbar]	3 [mbar]
Gravity pressure drop	82	88	105	108	64	83

Table 6.4: Pressure drop from gravity

Pressure drop from friction in straight pipes

Table 6.5 shows the predicted friction pressure drop from pressure drop models in straight pipes in chapter 4.3.

	Gathering Pipelines					
Models	12 [mbar]	4 [mbar]	6 [mbar]	26 [mbar]	16 [mbar]	3 [mbar]
Becker	122	157	127	73	13	531
Martinelli and Nelson	102	131	106	61	11	443
Friedel	94	127	109	61	11	462
Beattie	18	26	21	11	2	99
Lockhart and Martinelli	265	84	83	45	30	361
Baroczy	161	39	43	23	21	187
Wallis	48	57	49	26	5	229
Churchill	45	55	47	25	5	221
Grönnurud	262	227	206	109	28	949

Table 6.5: Pressure drop in straight pipes, Chisholm type c

Pressure drop from friction in bends

Table 6.6 shows the predicted friction pressure drop from pressure drop models in bends in chapter 4.3.1. An average value from equations 4.11, 4.16 and 4.16 is used. Only two models are in table 6.6 because Chisholm type b (2000) and P.Sookprasong models gave far too high pressure change.

	Gathering Pipelines					
	12	4	6	26	16	3
Models	[mbar]	[mbar]	[mbar]	[mbar]	[mbar]	[mbar]
Chisholm type c	148 [8]	61 [7]	42 [4]	25 [2]	13 [1]	290 [15]
Chisholm type b (1980)	235 [12]	120 [13]	84 [8]	47 [5]	19 [2]	625 [33]

Table 6.6: Pressure drop in bends, Chisholm type b (2010)

6.4.1 Total pressure drop

The total pressure drop consists of pressure drop by gravity and friction pressure drop in straight pipes and bends. Since there are two models for pressure drop in bends both scenarios will be examined and compared.
Table 6.7 shows the total pressure drop with Chisholm type c model as pressure drop in bends.

$$dP_{tot} = \Delta P_H + \Delta P_f + \Delta P_{fi,\text{Chisholm type c}} \tag{6.1}$$

	Gathering Pipelines					
	12	4	6	26	16	3
Models	[mbar]	[mbar]	[mbar]	[mbar]	[mbar]	[mbar]
Becker	353	306	274	207	90	906
Martinelli and Nelson	333	281	253	195	88	818
Friedel	325	276	256	194	88	837
Beattie	248	174	168	144	79	472
Lockhart and Martinelli	496	232	229	178	107	733
Baroczy	391	187	190	156	98	560
Wallis	279	206	196	159	82	603
Churchill	276	204	194	158	82	595
Grönnurud	492	376	353	243	105	1326

Table 6.7: Pressure drop in straight pipes

Table 6.8 shows the total pressure drop with Chisholm type b (1980) model as pressure drop in bends.

$$dP_{tot} = \Delta P_H + \Delta P_f + \Delta P_{fi,\text{Chisholm type b}} \tag{6.2}$$

Chisholm type b gives an average of 18% higher total pressure drop than Chisholm type c.

	Gathering Pipelines					
	12	4	6	26	16	3
Models	[mbar]	[mbar]	[mbar]	[mbar]	[mbar]	[mbar]
Becker	440	365	317	230	97	1242
Martinelli and Nelson	419	340	295	217	95	1154
Friedel	412	335	298	217	95	1172
Beattie	335	234	210	167	86	807
Lockhart and Martinelli	583	291	272	200	114	1069
Baroczy	478	246	232	179	105	896
Wallis	366	265	238	182	89	938
Churchill	363	263	236	181	88	930
Grönnurud	579	436	396	266	112	1661

Table 6.8: Pressure drop in straight pipes

6.5 Error

In this chapter the error in pressure drop models will be examined and average error with spread. Error in the pressure drop models were calculated using equation 6.3.

$$\text{Error } [\%] = \left| \frac{\text{Predicted value} - \text{Measured value}}{\text{Experimental result}} \right| \times 100 \tag{6.3}$$

The pressure drop models show a wide spread in error for their predictions for the gathering pipelines (see tables 6.11 for Chisholm type c and 6.12 for Chisholm type b). Therefor an average error was calculated with spread for each model using equation 6.4. The average error can be seen in tables 6.11, for Chisholm type c, and 6.12 for Chisholm type b.

$$\text{Average error } [\%] = \frac{1}{N} \sum_{1}^{N} \left| \frac{\text{Predicted value} - \text{Measured value}}{\text{Experimental result}} \right| \times 100 \tag{6.4}$$

	Gathering Pipelines					
	12	4	6	26	16	3
Models	[%]	[%]	[%]	[%]	[%]	[%]
Becker	14	53	37	1	40	71
Martinelli and Nelson	7	40	26	7	41	54
Friedel	5	38	28	8	41	58
Beattie	20	13	16	31	48	11
Lockhart and Martinelli	60	16	15	15	28	38
Baroczy	26	6	5	26	35	6
Wallis	10	3	2	24	45	14
Churchill	11	2	3	25	46	12
Grönnurud	59	88	77	16	30	150

Table 6.9: Error in pressure drop models
Chisholm type c

	Gathering Pipelines					
	12	4	6	26	16	3
Models	[%]	[%]	[%]	[%]	[%]	[%]
Becker	42	83	58	9	35	134
Martinelli and Nelson	35	70	48	4	37	118
Friedel	33	67	49	3	37	121
Beattie	8	17	5	20	43	52
Lockhart and Martinelli	88	46	36	5	24	102
Baroczy	54	23	16	15	30	69
Wallis	18	33	19	13	41	77
Churchill	17	32	18	14	41	76
Grönnurud	87	118	98	26	25	213

Table 6.10: Error in pressure drop models
Chisholm type b

Models	Average error [%]	spread [%]
Becker	36	± 56
Martinelli and Nelson	30	± 48
Friedel	30	± 50
Beattie	23	± 19
Lockhart and Martinelli	29	± 44
Baroczy	17	± 31
Wallis	16	± 30
Churchill	16	± 29
Grönnurud	70	± 90

Table 6.11: Average error in gathering pipelines Chisholm type c

Models	Average error [%]	spread [%]
Becker	60	± 85
Martinelli and Nelson	52	± 78
Friedel	52	± 79
Beattie	24	± 48
Lockhart and Martinelli	50	± 63
Baroczy	35	± 50
Wallis	33	± 59
Churchill	33	± 59
Grönnurud	95	± 119

Table 6.12: Average error in gathering pipeline Chisholm type b

6.6 Pressure drop with changing roughness

Pipe roughness is important in calculating the friction pressure drop. It is hard to assume the roughness without opening the pipe and measure it. With years of service, the pipelines roughness changes because of precipitation from the corrosive geothermal fluid. The average pressure drop in the gathering pipelines with changing pipe roughness is plotted in figure 6.6 for Chisholm type c and 6.6 for Chisholm type b. An average value for the measured pressure change in the gathering pipelines is also plotted as reference. It can be seen that with higher roughness the pressure drop rises. Though it is highly unlikely that the roughness will reach $10mm$.

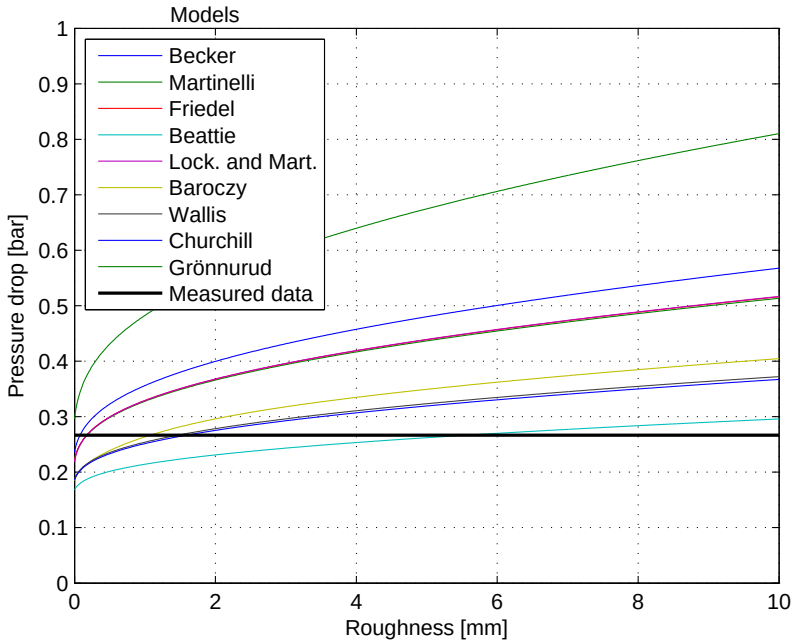

Figure 6.6: Pressure drop with changing roughness Chisholm type c

Table 6.13 shows the roughness in the pipe that gives the same pressure drop as measured according to pressure drop models, for Chisholm type c. There is no similar table for Chisholm type b, because even if the roughness is $0mm$ the predicted result never reaches the measured data.

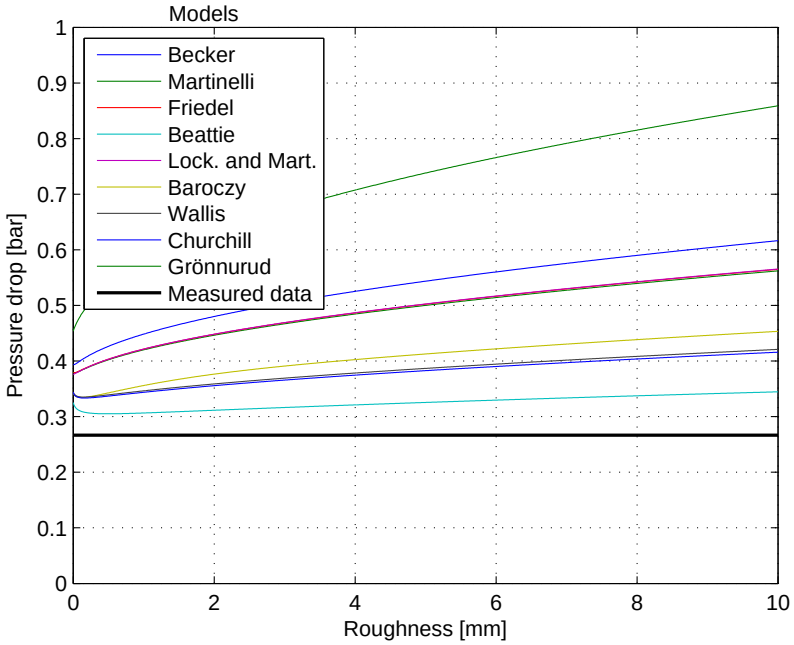

Figure 6.7: Pressure drop with changing roughness Chisholm type b

Models	Roughness [mm]
Becker	0.1
Martinelli and Nelson	0.17
Friedel	0.17
Beattie	5.6
Lockhart and Martinelli	0.17
Baroczy	1.1
Wallis	1.5
Churchill	1.6
Grönnurud	-

Table 6.13: Ideal roughness

7 Conclusion

The aim of this project was to measure pressure drop in gathering pipelines in the upper region of Hellisheiði power plant and compare measurements with known pressure drop models and choose a model which suits measured data. Six pressure measurements in gathering pipelines were made. Near the borehole and near the seperation station. More measurements should be made to be able to make another pressure drop model. But these measurements compared with the selected models can give a good accuracy of the models. Orkuveita Reykjavíkur and Mannvit h.f. provided the data of the gathering pipelines used in this project.

There are a few factors that must be addressed to be able to state the accuracy of the models.
Measurements error is a big factor in stating the accuracy. Measurements error in this projects are the reading and fluctuating of the manometer. The error in the manometer was $0.05bar$ and the fluctuating in the system gave a spread of the manometer of $0.1bar$.
Roughness in the pipelines is also a big factor for accuracy of the models. The roughness of the pipe is not known accurately since it is always changing because of the precipitation.
The data provided by Orkuveita Reykjavikur and Mannvit h.f. were all made at a different time and not made at the same time as the measurements in this project. With fluctuating in the system the most recent data might not give the best result.
The gathering pipelines in the upper region of Hellisheiði has a diameter of $1000mm$ which makes the comparison with the pressure drop models in this project hard, since the models selected in this project the research were made with a small diameter pipe. Most of them are $< 100mm$ in diameter which makes scaling these models up to the size in this project might not give an accurate results.

7.1 Comparison of models

Since the number of measurements made in this project were not many enough to be able to present a new model, it was decided to take a look at known pressure drop models and compare them to the measured data. 9 models were looked at for

straight pipes and 4 for bends. Of those 9 straight pipe models, 2 were pressure dependant and 7 were mass flux dependant.

Pressure dependant models

For the pressure dependant model Martinelli and Nelson model gave better result than Becker model. It gave about $13-17\%$ lower average error with $8-14\%$ lower spread in Chisholm type b and c models. Even if the average error in either model is not that far from the measured data, the spread is far too high to be acceptable.

Mass flux dependant models

For the mass flux dependant models Beattie model gave the best combined average error and spread. Even though Baroczy, Wallis and Churchill gave lower average error, the spread is higher. Grönnerud model gave the worst result, with very high average error and even higher spread. Lockhart and Martinelli model gives not accurate reading since the friction correction factor increases exponentionally with higher steam quality.

Bend models

4 bends models were looked at and Chisholm type b (1980) gave an average of 45% higher pressure drop than Chisholm type c. It is hard to compare these two models, which is better or worse, since they are compared in relation with the straight pipe models. With according to the straight pipe models the Chisholm type c gives the best result.

7.2 Future Work

When designing the pipe route in geothermal power plants, no one specific model is used but rather a route is selected in according to thermal expansions and landscape. The thermal expansion is calculated and a route which fits best to the landscape and with no low point and gives satisfactory expansion is selected. A better and more accurate way of doing this is to find a new pressure drop model.
Since most of the research in models presented in this model were made in a small

diameter pipe, $< 100m$, the models gave not accurate results compared with measure data. A new model for larger diameter pipes, as are used in geothermal power plants, is needed to be able to predict the pressure drop when designing the two phases flow pipe route. This would have to be done by increasing the measurement data points, not just by measuring more gathering pipelines but also more points on gathering pipelines so more measurements can be done on one gathering pipeline. Since the gathering pipelines in this project are $700 - 1300m$ long with a drop of $40 - 70m$, and with a roughness in the pipe which is not well known, the pressure drop models gives a wide spread in error. Measurements of pipe roughness must be made so the model can give an accurate result. Measuring pipe roughness with pipes in operation is impossible but the geothermal fluid must then be sent to the muffler at the borehole, then the gathering pipeline is empty, so the pipe roughness can be measured.

References

Awad, M., & Muzychka, Y. (2004). *A simple two-phase frictional multiplier calculation method.*

Azzi, Friedel, & Beladi. (2000). *Two-phase gas/liquid flow pressure loss in bends.*

Babcock, & WilcoxCo. (1978). *Steam: Its generation and use.*

Benjamin. (2013). *Improvement of pressure measurements in high temperature geothermal pipelines.*

Butterworth, D. (1974). *A comparison of some void-fraction relationships for co-current gas-liquid flow.*

Chisholm, D. (1973). *Pressure gradients due to friction during the flow of evaporating two-phase mixtures in smooth tubes and channels.*

Chisholm, D. (1983). *Two-phase flow in pipelines and heat exchangers.*

H.D. Zhao, K. L., & Freeston, D. (2000). *Geothermal two-phase flow in horizontal pipes.*

Hewitt. (1982). *The handbook of multiphase systems.* McGraw Hill.

Holmgren, M. (2010). *Water and steam properties according to iapws if-97* [Matlab function]. The MathWorks Inc.

Jayanti, S. (2011, feb). *Bends, flow and pressure drop in.* Retrieved from `http://www.thermopedia.com/content/577/`

Kiijarvi, J. (2011). *Darcy friction factor formulae in turbulent pipe flow.*

Þorbjörn Karlsson. (1979). *Nokkur atriði um tvífasa rennsli vatns og gufu.*

Pálsson, H. (2009). *Two phase flow – pressure drop.* Lecture notes.Univercity of Iceland.

Pálsson, H. (2012). *Simulation of two phase flow in a geothermal well.* Lecture notes.Univercity of Iceland.

Sigfússon, B., & Kjartansson, G. (2013). *Afl og afkastageta gufuhola á hellisheiði.*

Speeding. (1996). *Prediction in stratified gas-liquid co-current flow in horizontal pipelines.*

Zivi. (1964). *Estimation of steady state steam void fraction by means of the principle of minimum entropy production.*